Targeting PARG induces tumor cell growth inhibition and antitumor immune response by reducing phosphorylated STAT3 in ovarian cancer

Antons Martincuks,[1] Chunyan Zhang,[1] Theresa Austria,[1] Yi-Jia Li ![ORCID] ,[1] Rui Huang,[1] Nicole Lugo Santiago,[2] Adrian Kohut,[2] Qianqian Zhao,[1,3] Rosemarie Martinez Borrero,[1,3] Binghui Shen,[4] Mihaela Cristea,[5] Edward W Wang,[5] Mihae Song,[2] Lorna Rodriguez-Rodriguez,[2] Hua Yu ![ORCID] [1]

Correspondence to
Dr Hua Yu; HYu@coh.org

Lorna Rodriguez-Rodriguez; lorrodriquez@coh.org

ABSTRACT

Background Ovarian cancer is the most lethal gynecological malignancy, with limited treatment options after failure of standard therapies. Despite the potential of poly(ADP-ribose) polymerase inhibitors in treating DNA damage response (DDR)-deficient ovarian cancer, the development of resistance and immunosuppression limit their efficacy, necessitating alternative therapeutic strategies. Inhibitors of poly(ADP-ribose) glycohydrolase (PARG) represent a novel class of inhibitors that are currently being assessed in preclinical and clinical studies for cancer treatment.

Methods By using a PARG small-molecule inhibitor, COH34, and a cell-penetrating antibody targeting the PARG's catalytic domain, we investigated the effects of PARG inhibition on signal transducer and activator of transcription 3 (STAT3) in OVCAR8, PEO1, and *Brca1*-null ID8 ovarian cancer cell lines, as well as in immune cells. We examined PARG inhibition-induced effects on STAT3 phosphorylation, nuclear localization, target gene expression, and antitumor immune responses in vitro, in patient-derived tumor organoids, and in an immunocompetent *Brca1*-null ID8 ovarian mouse tumor model that mirrors DDR-deficient human high-grade serous ovarian cancer. We also tested the effects of overexpressing a constitutively activated STAT3 mutant on COH34-induced tumor cell growth inhibition.

Results Our findings show that PARG inhibition downregulates STAT3 activity through dephosphorylation in ovarian cancer cells. Importantly, overexpression of a constitutively activated STAT3 mutant in tumor cells attenuates PARG inhibitor-induced growth inhibition. Additionally, PARG inhibition reduces STAT3 phosphorylation in immune cells, leading to the activation of antitumor immune responses, shown in immune cells cocultured with ovarian cancer patient tumor-derived organoids and in immune-competent mice-bearing mouse ovarian tumors.

Conclusions We have identified a novel antitumor mechanism underlying PARG inhibition beyond its primary antitumor effects through blocking DDR in ovarian cancer.

WHAT IS ALREADY KNOWN ON THIS TOPIC

⇒ Poly(ADP-ribose) glycohydrolase (PARG) enzyme, which facilitates DNA repair by dismantling PAR polymers on proteins, is pivotal in cellular function and DNA damage response (DDR), and its blockade by small-molecule inhibitors, induces DDR-deficient tumor cell death in vitro and in vivo.

WHAT THIS STUDY ADDS

⇒ In this study, we demonstrate that targeting PARG provokes tumor cell growth inhibition not only through regulating DDR, but also by inhibiting a pro-oncogenic and immunosuppressive transcription factor signal transducer and activator of transcription 3 (STAT3) via dephosphorylation in tumor cells. Importantly, we show that PARG inhibition also decreases STAT3 phosphorylation in immune cells, inducing antitumor immune responses in vitro, and in ovarian cancer patient tumor-derived organoid-immune cell cocultures, as well as in immuno-competent mice harboring DDR-deficient ovarian tumors.

HOW THIS STUDY MIGHT AFFECT RESEARCH, PRACTICE OR POLICY

⇒ This study unveils a novel mechanism: PARG inhibition may be a promising strategy to inhibit STAT3 and enhance antitumor immune responses, which may also enhance the efficacies of other immunotherapies. Our findings compellingly advocate for the clinical development of PARG inhibitors for cancer treatments, including potential combinatory strategies with immunotherapies for ovarian cancer and other malignancies.

Furthermore, targeting PARG activates antitumor immune responses, thereby potentially increasing response rates to immunotherapy in patients with ovarian cancer.

BACKGROUND

Ovarian cancer significantly contributes to cancer-related mortality among women worldwide, with high-grade serous ovarian cancer (HGSOC) being the most common and aggressive subtype.[1 2] Despite advances in surgical and chemotherapeutic treatments, the prognosis for advanced-stage HGSOC remains poor.[2] Although immunotherapies, such as immune checkpoint blockades, have demonstrated substantial clinical benefits for various cancer types, they have only modest responses in ovarian cancer.[3] Emerging evidence indicates that the immune cells in the ovarian cancer microenvironment are highly suppressed, contributing to the ineffectiveness of immune checkpoint blockades.[4 5] Consequently, there is a crucial need to develop novel therapeutic strategies to combat immunosuppression in ovarian cancer.

Poly(ADP-ribose) polymerase (PARP) inhibitors (PARPis) are a class of small-molecule inhibitors that prevent the repair of DNA single-strand breaks by inhibiting the PARP enzyme, which mediates poly-ADP-ribosylation (PARylation) of target proteins.[6 7] PARPis have demonstrated significant clinical activity in patients with ovarian cancer, particularly those with defects in the DNA damage response (DDR) pathway.[8] However, most patients treated with PARPis eventually develop drug resistance.[9]

Recently, several studies have reported that PARPis inadvertently activate signal transducer and activator of transcription 3 (STAT3) by increasing its phosphorylation in both tumor and immune cells, thereby contributing to acquired PARPi resistance and immunosuppression in ovarian cancer.[10 11] Moreover, it has been suggested that STAT3 activation induced by PARP inhibition is mediated through dePARylation.[12] In addition to PARPi resistance development, we and others have demonstrated a critical role of STAT3 intrinsic to immune cells in compromising antitumor immunity, and targeting STAT3 activates antitumor immune responses.[13–16]

Poly(ADP-ribose) glycohydrolase (PARG) is an enzyme that reverses the PARylation process by breaking down long chains of PAR polymers on proteins, thus having an opposite function to PARP.[17] Rather than antagonizing PARylation, PARG-mediated dePARylation serves as a critical downstream step of PARylation in DDR. Specifically, PARG plays a vital role in cellular function by facilitating DNA single-strand and double-strand break repair, releasing DDR factors from PARylation chains at damaged sites, and enabling proper repair mechanisms.[18] Therefore, blocking PARG also induces tumor cell death, especially in cells defective in DDR. Several PARG inhibitors (PARGis) have been recently developed and show promising potential for cancer therapy as monotherapy or in combination with other cytotoxic agents or radiation in vitro and in animal tumor models.[19 20] Among them, COH34 is a potent, specific, and cell-permeable PARGi that has exhibited greater synthetic lethality potential in both DDR-deficient cells and PARPi (olaparib)-resistant cells.[20] However, the effects of PARG inhibition on antitumor immune responses and the underlying mechanisms remain unknown.

In this study, we discovered that targeting PARG inhibits STAT3 signaling in both mouse and human ovarian cancer tumor cells and tumor-associated immune cells. Additionally, we demonstrated that PARG inhibition induces activation of antitumor immune responses, and tumor cell death mediated by the downregulation of STAT3 signaling in addition to modulating DDR. These findings provide critical insight into the relationship between PARG and STAT3 in ovarian cancer and establish a rationale for developing PARG inhibitors in combination with immunotherapies.

METHODS

Patient ovarian tumor specimens

An honest broker at City of Hope screened patients with advanced stage ovarian cancer undergoing cytoreductive surgery. Peripheral blood and tumor tissue samples were obtained from three patients diagnosed with HGSOC, at stages IIIC–IVA. The patient's ages were between 37 and 58 years. The specimens, after undergoing pathological evaluation by City of Hope pathology lab, were then deidentified, processed for further analyses under institutionally approved protocols.

Mice

In our study, we conducted three experiments using a total of 56 female C57BL/6 mice, aged 7–8 weeks, purchased from Jackson Laboratory. We performed mouse care and experimental procedures under pathogen-free conditions in accordance with established institutional guidance and approved protocols from the Institutional Animal Care and Use Committee (#23045) at the Beckman Research Institute of City of Hope National Medical Center. All mice were housed in the Animal Resource Center (ARC) of Beckman Research Institute/City of Hope under the care of veterinarians. For housing, we accommodated five mice per cage, with a minimum cage height of 5 inches and a floor area of 15 inches squared per mouse. The environmental conditions were carefully regulated: the temperature was maintained between 68°F and 75°F (20-24°C) with relative humidity levels of 30%–70%. A 12-hour light/dark cycle was strictly followed. Mice had free access to a general diet and water. For enrichment, nesting materials and toys were provided in the cages. Prior to experimental procedures, the mice underwent a 7-day acclimation period in the ARC. No additional specific preparations were conducted.

In vivo mouse studies

In this study, we used anti-mouse CD8α (clone 53-6.72) monoclonal antibody (mAb) and isotype control rat IgG 2b (BioXcell) for in vivo depletion of CD8+ T cell experiments. Three days before injecting *Brca1*-null ID8 tumor cells, we administered anti-mouse CD8α mAb (0.1 mg/mouse) or rat IgG2b control (0.1 mg/mouse) to mice

through intraperitoneal injection once a day for three consecutive days. We confirmed that the efficacy of CD8^{+} T cell depletion is >98% by flow cytometry, as described previously.[21]

We injected *Brca1*-null ID8 mouse ovarian tumor cells (5×10^6) subcutaneously into CD8^{+} T cell-depleted and IgG treated control mice (n=14 for both groups). When the tumors reached an average size of $100 \, mm^3$ (day 5), mice with similar average tumor size were randomly divided into four groups (n=7). We treated tumor-bearing mice with or without CD8^{+} T cell-depletion with either vehicle control (30% solutol and 0.1% dimethyl sulfoxide (DMSO)) or COH34 (20 mg/kg in 30% solutol and 0.1% DMSO) daily by intraperitoneal injection for 7 days.

Throughout the experiments, mice were monitored every other day for health and well-being. In case of adverse symptoms, the protocol mandates immediate euthanasia. Tumor growth and discomfort levels were also closely monitored, with daily checks implemented near humane endpoints. Euthanasia was conducted using CO_2, adhering to stringent ethical guidelines. This included confirmation of death by cessation of breathing and no response to tail pinch, with a secondary method of euthanasia (cervical dislocation) employed if necessary.

After euthanizing the mice, we harvested and weighed their tumors for further analysis. To prepare single-cell suspensions, we dissected tumor tissues into approximately $1–5 \, mm^3$ fragments and digested them with Collagenase D (2 mg/mL; Roche, 11088882001) and DNase I (1 mg/mL; Roche, 04716728001) for 30–45 min at 37°C. We filtered the digests through 70–100 µm cell strainers and centrifuged them at 1500 rpm for 5 min. After red blood cell lysis (Sigma-Aldrich, R7757), we filtered, washed, and resuspended single-cell suspensions in a flow buffer before flow cytometry analyses.

Ovarian cancer patient tumor tissue processing

We processed fresh ovarian tumor biopsies as previously described.[22] Briefly, we sectioned ovarian cancer patient tumor tissues into $3–5 \, mm^3$ pieces on arrival. We stained two or three random pieces for immunofluorescence, while processing the remaining tissue for organoid derivation. To obtain organoids, we minced and digested the tissue in Hank's Balanced Salt Solution containing Collagenase D and DNase I at 37°C for 0.5–1.5 hour. After straining the digested suspension through a 100 µm filter and centrifuging, we added erythrocyte lysis buffer to any visible red pellet for 5 min at room temperature and repeated washing steps. We isolated patient-matched peripheral blood mononuclear cells (PBMCs) from peripheral blood using Ficoll-Paque density gradient separation and cryopreserved them for future use.

Organoid culture

We cultured air–liquid interface patient-derived tumor organoids (ALI-PDTOs) as described previously.[23] We placed 0.4 µm 30 mm diameter inserts (transwells) with permeable, membranous bottoms (PIHP03050, Millicell,

Millipore) into six-well plates. We added Collagen Gel Matrix (CGM,[23] see online supplemental methods 1) to each insert and incubated them at 37°C for 30 min to solidify. We resuspended processed ovarian cancer tissue pellets in CGM at 5,00,000–1,000,000 cells/mL and layered 1 mL of this suspension on the presolidified gel in the transwell. We placed the transwell in a six-well plate containing 1.0 mL of ovarian organoid medium (OOM,[22] see online supplemental methods 2) supplemented with 500 IU/mL recombinant human interleukin-2 (IL-2, Peprotech). We cultured ALI-PDTOs for 30–60 days until visible spheroids formed and changed the medium twice weekly.

Statistical analysis

Experiments were conducted at least two times independently, and statistical significance was evaluated using GraphPad Prism V.7 or V.8 software, with a $p<0.05$ considered significant. The sample size was not predetermined, and data were analyzed by two-tailed Student's t-test. All results are presented as mean±SD, unless stated otherwise. No blinding methods were used during data collection and analysis; normal data distribution was presumed.

RESULTS
PARG inhibition decreases STAT3 Y705 phosphorylation and signaling

To determine whether targeting the dePARylation enzyme PARG has the opposite effect on STAT3 phosphorylation (pSTAT3) compared with PARP inhibition,[10–12] we selected the PEO1, *Brca1*-null ID8, and OVCAR8 cell lines for their diverse DDR status. The BRCA2-deficient PEO1 line, previously tested for its response to COH34,[20] and the syngeneic mouse *Brca1*-null ID8 line, developed for studying antitumor immune responses,[24] serve as DDR-deficient models. In contrast, the OVCAR8 line, initially characterized by *BRCA1* promoter methylation and reduced BRCA1 expression,[25] demonstrates PARPi resistance and DDR competence,[26] providing a valuable comparison to the DDR deficiency observed in PEO1 and *Brca1*-null ID8. We treated OVCAR8, PEO1, and *Brca1*-null ID8 ovarian cancer cell lines with either 10 µM olaparib (PARPi) or COH34 (PARGi) and assessed the levels of phosphorylated STAT3. As reported before, treatment of cells with the PARPi, olaparib, led to increased pSTAT3 and reduced total PARylation by 40%–70%. In stark contrast, treatment with a PARGi resulted in a 50%–70% reduction in pSTAT3 levels and a 1.9–2.1 fold increase in total PARylation (figure 1A). Co-immunoprecipitation experiments further demonstrated that PARGi treatment increased STAT3 PARylation in the tumor cells by approximately 60% (online supplemental figure 1A). Additionally, we observed a significant reduction in pSTAT3 by PARGi in triple-negative breast cancer and pancreatic cancer cell lines (online supplemental figure 1B).
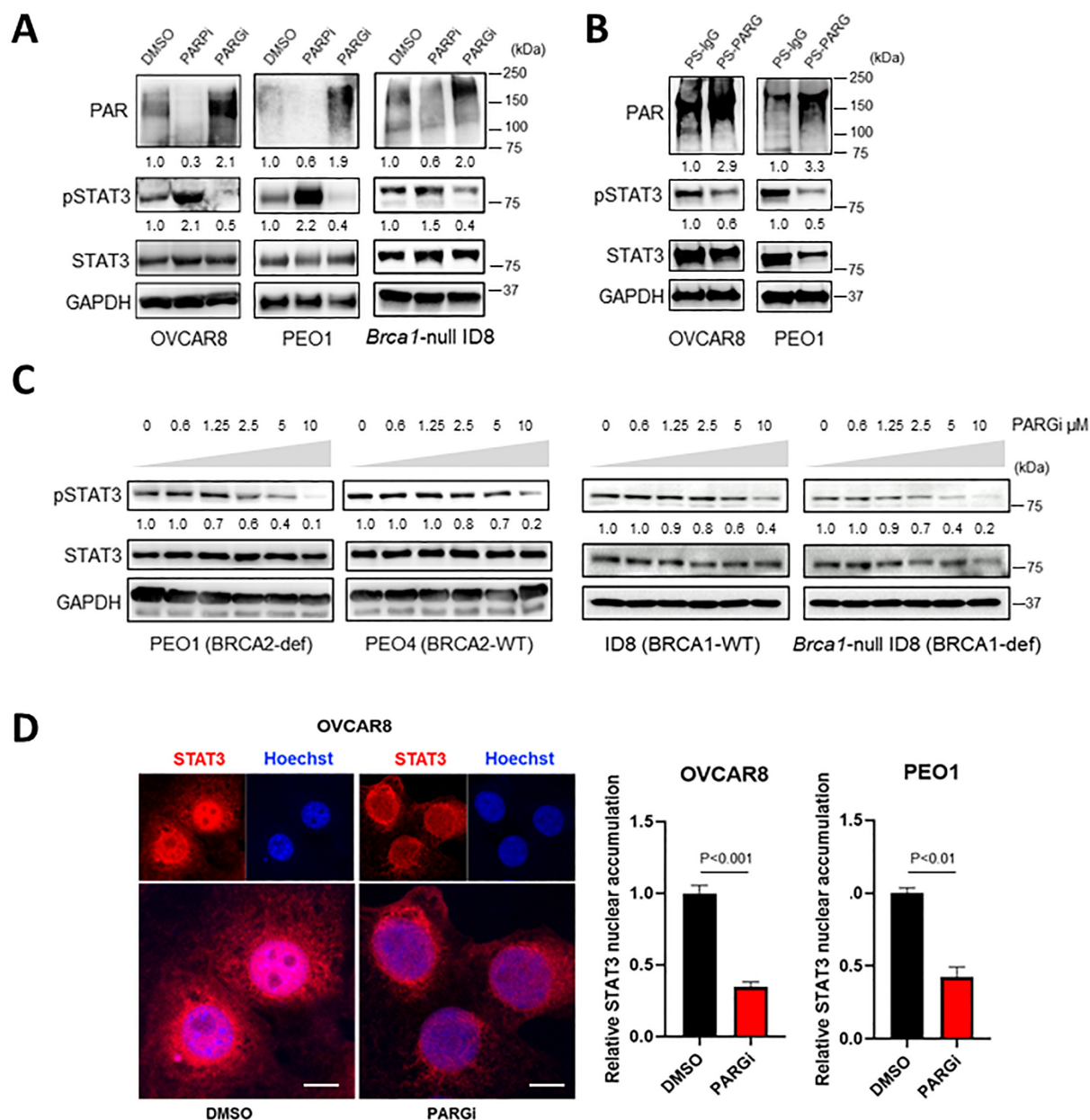
Figure 1 PARG inhibition decreases STAT3 Y705 phosphorylation and signaling. (A) Immunoblot analysis comparing total PARylation, phospho-STAT3 Tyr 705 (pSTAT3), total STAT3 (STAT3), and loading controls in BRCA-proficient OVCAR8, BRCA2-deficient PEO1, and *Brca1*-null ID8 cells after vehicle (DMSO), 10 µM olaparib (PARPi), or 10 µM COH34 (PARGi) overnight incubation. The image represents three independent experiments. (B) Immunoblotting of the indicated cell lines cultured with the PS-modified control (PS-IgG) or PARG (PS-PARG) antibody (20 µg/mL, overnight). The image represents two independent experiments. (C) Dose-dependent pSTAT3 inhibition by COH34 at indicated doses in BRCA-proficient and BRCA-deficient ovarian cancer cells analyzed by immunoblotting. The images represent two independent experiments. GAPDH was used as the loading control. (D) Immunofluorescent staining and confocal microscopic images (left) showing STAT3 (red) and nuclear staining (blue) of the indicated ovarian cancer cell lines treated with DMSO or 10 µM PARGi overnight. The scale bars represent 10 µm. Histograms (right) showing STAT3 nuclear accumulation. Data shown are mean±SD from three experiments. The protein levels of PAR or pSTAT3 shown in the immunoblotting images were quantified by band intensity using ImageJ software and normalized with GAPDH. DMSO, Dimethyl sulfoxide; GAPDH, Glyceraldehyde 3-phosphate dehydrogenase; PARG, poly(ADP-ribose) glycohydrolase; STAT3, signal transducer and activator of transcription 3.

To further validate our findings, a different approach that blocks PARG more specifically was used: we employed cell-penetrating antibodies that are modified by phosphorothioated DNA oligonucleotides[27] (PS-PARG) to block PARG at its catalytic domain. Treating tumor cells with the PS-PARG antibody induced similar cytotoxic effects as PARG inhibition by COH34 observed in an earlier study,[20] and as shown in online supplemental figure 1C. Compared

with control PS-IgG antibody treatment, PS-PARG antibodies efficiently bound to endogenous PARG enzymes, as demonstrated by Protein A immunoprecipitation (online supplemental figure 1D), and PS-PARG antibodies colocalized with PARG in the nuclei of ovarian cancer cells (online supplemental figure 1E). Moreover, PS-PARG antibody treatment, like COH34, reduced pSTAT3 by 40%–50% and increased total PARylation by 2.9–3.3 fold (figure 1B). In addition, doses ranging from 0.6 to 10 μM of PARGi showed a dose-dependent effect on pSTAT3 levels in both BRCA-deficient and BRCA-proficient cells (figure 1C), suggesting that PARGi antitumor effects may not be restricted to DDR-deficient cells.

We further investigated whether the reduced pSTAT3 could lead to a decrease in STAT3 signaling by determining STAT3 nuclear localization in ovarian cancer cells on PARGi treatment. Immunofluorescent staining and confocal microscopy analysis revealed a notable reduction, at least 50%, in nuclear STAT3 following PARGi treatment compared with DMSO control (figure 1D). Collectively, our results show opposing effects of PARG inhibition on STAT3 signaling compared with PARPi, raising the possibility that PARG may be a more effective target than PARP in the treatment of ovarian cancer.

PARGi-induced tumor cell growth inhibition is partially mediated by blocking STAT3

We next determined whether blocking PARG could inhibit the expression of known STAT3 target genes involved in tumor cell survival and metastasis. After treating BRCA-proficient OVCAR8 and BRCA2-deficient PEO1 ovarian cancer cell lines with 10 μM PARGi for 24 and 48 hours, we observed a notable downregulation of several STAT3 target genes. In OVCAR8 cells, the expression of Bcl-xL and Survivin was significantly decreased at 24 hours, with this reduction becoming even more pronounced at 48 hours. Similarly, in PEO1 cells, the expression levels of MMP2, MMP9 and Bcl-xL showed a decline following PARGi treatment, aligning with the observed pattern in OVCAR8 cells (figure 2A).

To further investigate the role of STAT3 in mediating PARGi-induced tumor cell growth inhibition, we ectopically expressed STAT3C, a constitutively activated mutant of STAT3,[28] in ovarian cancer cells. Overexpressing STAT3C in OVCAR8, PEO1, and *Brca1*-null ID8 ovarian cancer cell lines, verified via immunoblotting (figure 2B), increased the number of viable colonies in PARGi (5 μM)-treated cells by 2–5 fold compared with mock controls, as shown in colony formation assays (figure 2C,D). Moreover, in our dose-response cell viability assays with PARGi, we observed a statistically significant increase in survival of tumor cells expressing STAT3C (figure 2E). Specifically, OVCAR8 cells transfected with STAT3C exhibited a 1.8-fold increase in IC_{50} (22.31 μM for STAT3C vs 12.39 μM for mock). Similarly, PEO1 cells with STAT3C showed a 2.96-fold increase in IC_{50} (25.59 μM for STAT3C vs 8.66 μM for mock) and *Brca1*-null ID8 cells demonstrated a 2.12-fold increase (25.01 μM for STAT3C vs 11.81 μM

for mock). These findings suggest that tumor cell growth inhibition induced by PARGi is partially abrogated by restoring STAT3 signaling, pointing to the potential of PARG targeting in supressing growth of tumor cells, irrespective of BRCA status.
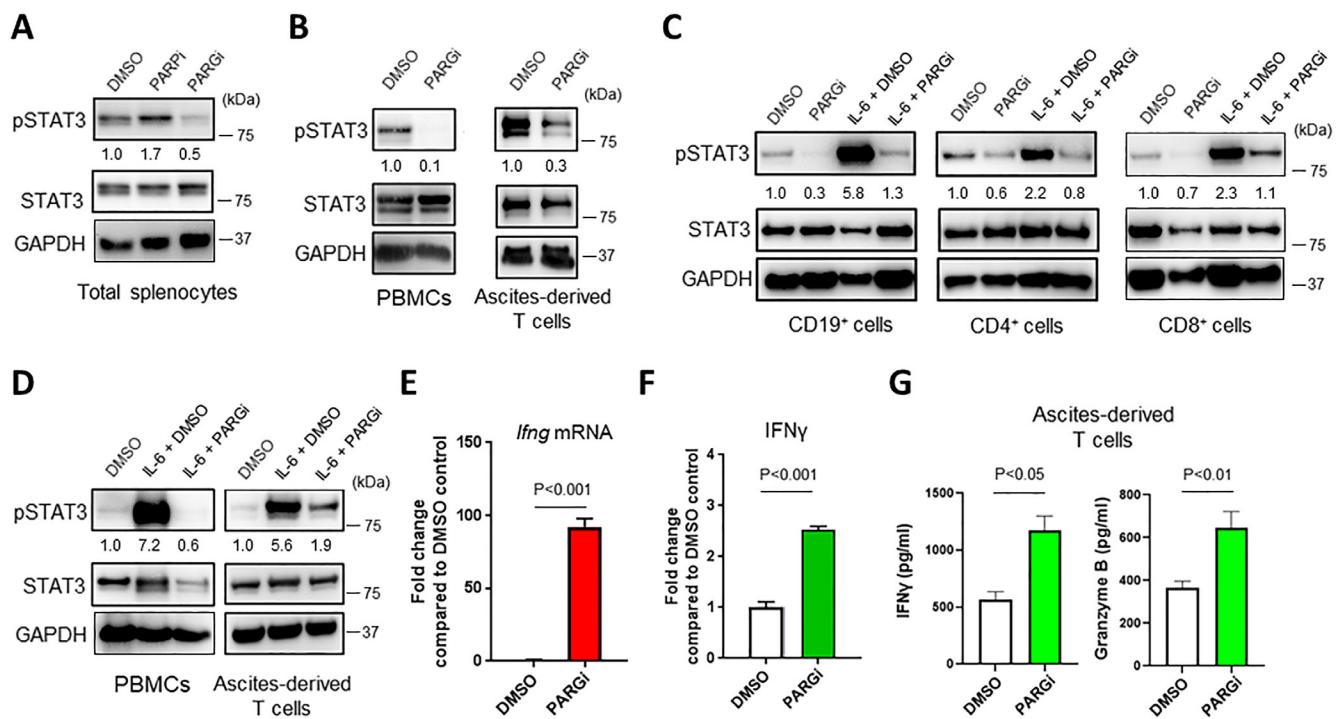
PARG inhibition decreases pSTAT3 in immune cells and activates immune responses

To investigate whether PARG inhibition has a similar inhibitory effect on pSTAT3 in immune cells observed in ovarian cancer cells, we treated freshly isolated splenic cells from tumor-free mice with 10 μM of either PARPi (olaparib) or PARGi (COH34). Immunoblotting showed that PARGi significantly reduced pSTAT3, even at lower 1.25–5 μM concentrations (online supplemental figure 2A), in contrast to the increase induced by PARPi (figure 3A). This effect was replicated in human immune cells, where 5 μM PARGi lowered basal pSTAT3 by 70%–90% in both healthy donor PBMCs and ovarian cancer patient-derived T cells activated by αCD3/αCD28 antibodies (figure 3B). Elevated pSTAT3-positive B cells, CD4+ and CD8+ T cells were previously observed in the tumor tissues derived from PARPi-resistant patients with ovarian cancer.[11] Pretreatment with 5 μM PARGi overnight reduced basal pSTAT3 and prevented IL-6-induced pSTAT3 in mouse CD19+ B cells and CD4+ or CD8+ T cells (figure 3C). Confirming these findings, PARGi pretreatment inhibited IL-6 induced pSTAT3 in human PBMCs and in activated T cells (figure 3D). Additionally, PS-PARG antibody treatments showed comparable decreases in pSTAT3 in both mouse and human T cells (online supplemental figure 2B,C). These results collectively underscore the inhibitory effect of PARG targeting on pSTAT3 across diverse immune cell types.

Interferon-gamma (IFNγ) and granzyme B are well-established immunostimulatory and antitumor effectors produced by cytotoxic T cells,[29 30] and their expression is negatively regulated by STAT3.[31 32] To determine if PARG inhibition leads to immunostimulatory effects, we analyzed *Ifng* mRNA expression in mouse splenic cells treated with 10 μM PARGi for 24 hours. Quantitative RT-PCR revealed a significant increase in *Ifng* expression (p<0.001) relative to unstimulated mouse splenic immune cells (figure 3E). Additionally, ELISA analyses of cocultures of mouse CD8+ T cells with ID8 tumor cells revealed 2.5-fold increase (p<0.001) in IFNγ production following PARGi treatment (figure 3F), which correlated with significant pSTAT3 reduction (online supplemental figure 2D). Similarly, in ovarian cancer patient-derived T cells treated with 5 μM PARGi, ELISA detected significantly increased IFNγ (p<0.05) and granzyme B (p<0.01) levels compared with controls (figure 3G). Additionally, blocking PARG with PS-PARG antibody in the patient ascites-derived T cells also elevated IFNγ production, relative to untreated or PS-IgG treated samples (online supplemental figure 2E). These findings collectively suggest that PARG blockade in immune cells not only
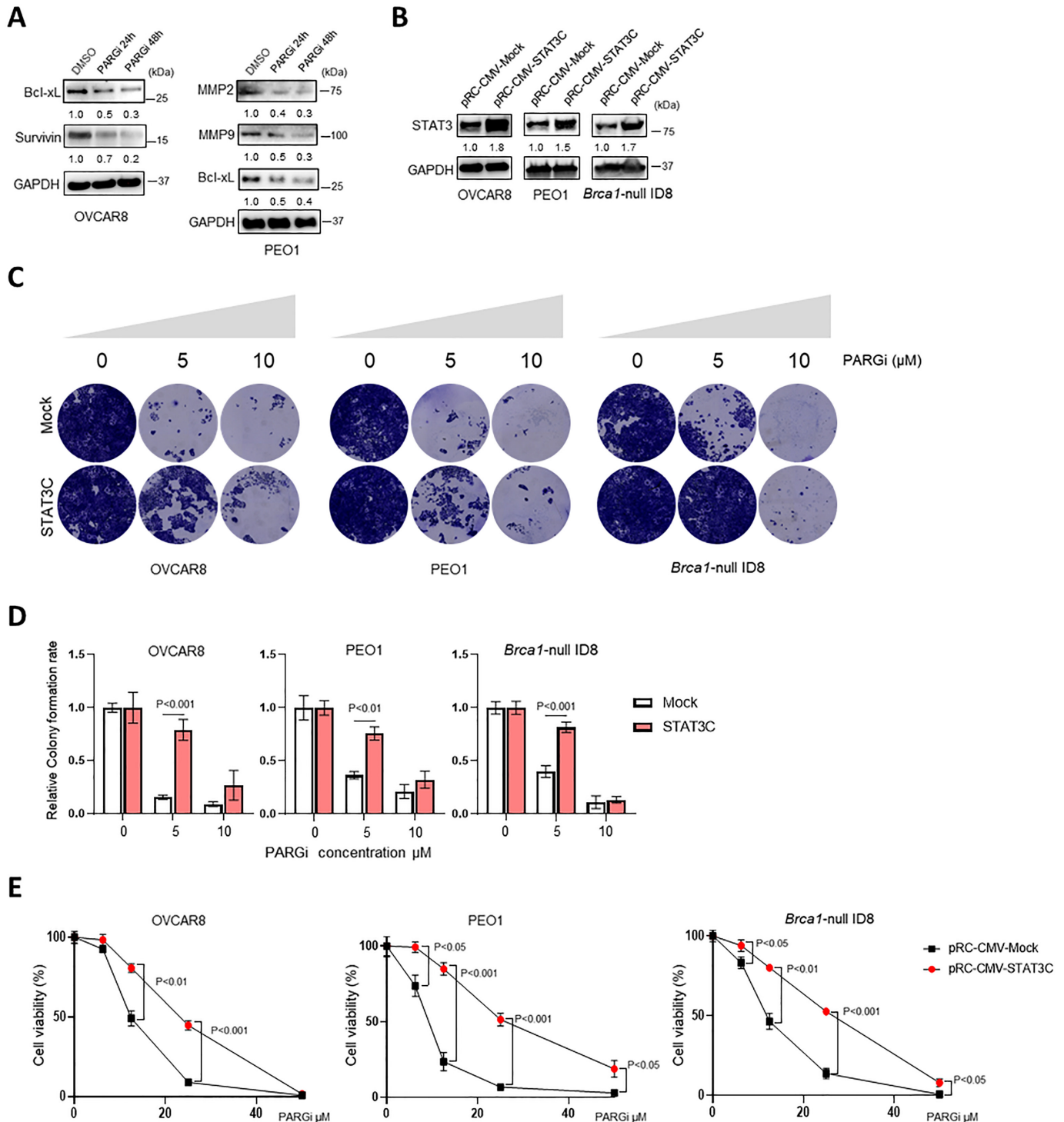
Figure 2 PARGi-induced tumor cell growth inhibition is partially mediated by blocking STAT3. (A) A representative immunoblot of STAT3 downstream genes and loading controls in ovarian cancer cells treated with 10 µM COH34 at indicated time points. The experiment was performed twice. (B) Immunoblot comparing total STAT3 and loading controls in ovarian cancer cell lines transfected with either control vector (Mock) or constitutively active form of STAT3 (STAT3C). The image represents two independent experiments. (C) Representative colony formation assays of Mock transfected and STAT3C transfected cells from (B) in the presence of PARGi at indicated concentrations for 10 days. Images represent three independent experiments. (D) Relative colony-formation by the indicated Mock and STAT3C transfected ovarian cancer cell lines treated with increasing concentrations of COH34 (0 µM, 5 µM and 10 µM). (E) Cell viability analysis of the Mock transfected and STAT3C transfected ovarian cancer cell lines. Cells were treated with indicated concentrations of COH34 for 3 days (0, 6.25, 12.5, 25, and 50 µM). Error bars represent mean±SD of n=3 independent experiments, two-tailed, unpaired Student's t-test. The protein levels of Bcl-xL, Survivin, MMP2, MMP9 or total STAT3 shown in the immunoblotting images were quantified by band intensity using ImageJ software and normalized with the levels of GAPDH. PARG, poly(ADP-ribose) glycohydrolase; STAT3, signal transducer and activator of transcription 3.

Figure 3 PARG inhibition (PARGi) decreases basal and IL-6-induced phosphorylated STAT3 (pSTAT3) in immune cells and stimulates immune activation in vitro. (A) Splenocytes from tumor-free mice were isolated and cultured in the presence of vehicle (DMSO), 10 μM olaparib (PARPi), or 10 μM COH34 (PARGi) overnight. The levels of pSTAT3 and total STAT3 were analyzed by immunoblotting. (B) Immunoblot comparing pSTAT3 in healthy donor-derived PBMCs and ovarian cancer patient ascites-derived CD3$^+$ T cells after overnight incubation with either DMSO or 5 μM PARGi. (C) Immunoblotting of pSTAT3 in mouse naïve CD19$^+$ B cells, CD4$^+$ and CD8$^+$ T cells pretreated with vehicle control or PARGi (5 μM, overnight) and stimulated with 20 ng/mL IL-6 for 30 min. (D) Analysis of IL-6-induced pSTAT3 similar to (C) in human immune cells from (B) after overnight pretreatment with either DMSO or 5 μM PARGi. (E) Real-time PCR of *Ifng* gene expression in mouse splenocytes cultured in the presence or absence of PARGi for 24 hours. Gene expression data are shown after normalization to *Actb* expression and are presented as the mean-fold induction (mean±SD) relative to unstimulated samples. (F) ELISA measuring IFN-γ levels in the supernatants from cocultures of mouse CD8$^+$ T cells with murine ID8 tumor cells in the presence of vehicle or 10 μM PARGi for 24 hours. Data are presented as the mean-fold induction (mean±SD) relative to vehicle-treated samples. (G) Levels of IFN-γ and granzyme B in the supernatants from ovarian cancer patient ascites-derived CD3$^+$ T cells after treatment with either 5 μM PARGi or DMSO for 24 hours as determined by ELISA. The protein levels of pSTAT3 shown in the immunoblotting images were quantified by band intensity using ImageJ software and normalized with the levels of GAPDH. DMSO, Dimethyl sulfoxide; GAPDH, Glyceraldehyde 3-phosphate dehydrogenase; PARG, poly(ADP-ribose) glycohydrolase; PBMCs, peripheral blood mononuclear cells; STAT3, signal transducer and activator of transcription 3.

diminishes pSTAT3 but also elevates immunostimulatory molecules.

PARG inhibition induces immune activation in ovarian cancer patient-derived tumor organoids

We next investigated the effects PARG inhibition on immune responses in the ovarian cancer patient tumor microenvironment. We used ALI-PDTOs, cultured from tumors from three stages IIIC-IVA patients with ovarian cancer for 30–60 days. The ALI-PDTOs, mirroring the tumor's three-dimensional architecture,[23] were cocultured with patient-matched autologous PBMCs, and treated with PARG targeting agents, followed by collecting the supernatants for ELISA and cell lysates for immunoblotting analyses, to evaluate immune response modulation by PARG inhibition (figure 4A). Histological comparisons using PAX8 and p53 staining confirmed

the consistency of ALI-PDTO markers with the original tumor tissues (online supplemental figure 3).

Immunoblotting analysis of both ALI-PDTOs, and PBMCs from autologous ovarian cancer patient-derived organoid/PBMC cocultures, treated with PARGi and PS-PARG antibodies showed a 50%–70% reduction in pSTAT3 compared with DMSO and PS-IgG controls, respectively (figure 4B). It is noteworthy that although cells treated with PARG inhibitors exhibited a decrease in both pSTAT3 and total STAT3 levels, activated STAT3 can positively regulate its own expression under certain conditions.[33 34] Additionally, we quantitatively assessed cytokine levels in the coculture supernatants by ELISA. Our results showed that either PARGi or PS-PARG antibody treatment led to a 2.8–3.5 fold increase in the immunostimulatory cytokines IFN-γ and granzyme B, along
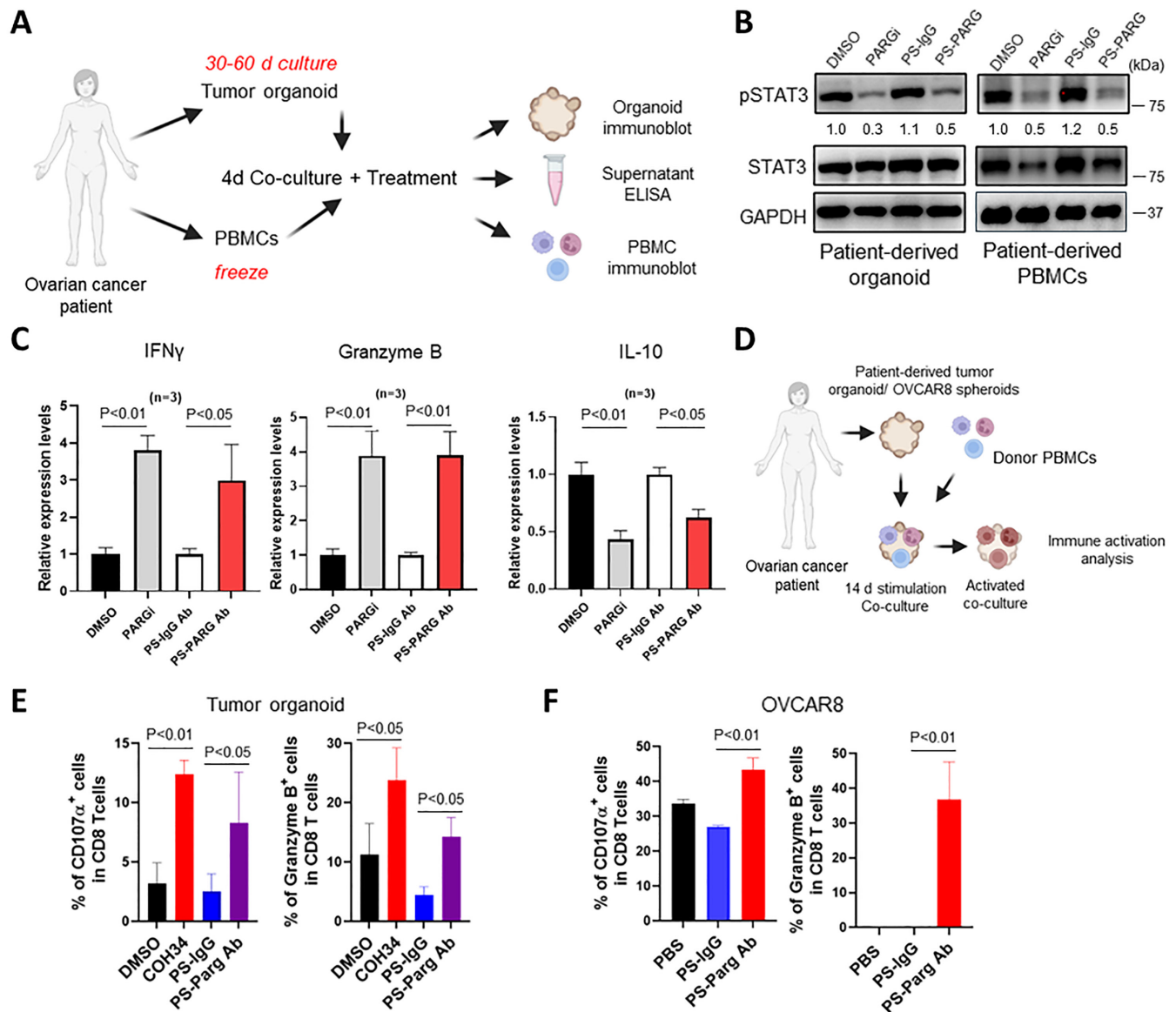
Figure 4 PARG inhibition induces immune activation in ovarian tumor organoids. (A) Study design for (B,C) from ovarian cancer patient-derived tumor organoid/PBMC cocultures in the presence of 0.1% DMSO and 10 µM COH34 (96 hours), or 20 µg/mL PS-IgG and PS-PARG antibodies (48 hours). (B) Immunoblotting of phosphorylated STAT3 (pSTAT3) in ovarian cancer PDOs and patient-matched PBMCs after the PDO/PBMC cocultures were treated by DMSO, COH34, PS-IgG or PS-PARG antibodies. Data are representative of three independent experiments. (C) IFN-γ, granzyme B, and IL-10 levels in the PDO/PBMC coculture supernatants as measured by ELISA. Expression data are presented as mean-fold induction (mean±SD) relative to control samples from three different patients. (D) Study design for (E,F). PDOs or OVCAR8 spheroids and healthy donor PBMCs were prepared separately before coculturing. Tumor organoids (E) or OVCAR8 tumor cells (F) were cocultured with healthy donor PBMCs for 72 hours in the presence of 0.1% DMSO, 10 µM COH34, PS-IgG, or PS-PARG antibodies. Single-cell suspensions prepared from the cocultures of tumor organoids or OVCAR8 tumor cells and healthy donor PBMCs were analyzed by flow cytometry for activated T cells (GzmB+ or CD107a+) in CD8+ T cell populations. For tumor organoids, n=4; and for OVCAR8 tumor cells, n=3 (n represents the number of PBMC donors). The protein levels of pSTAT3 in the immunoblotting images were quantified by band intensity using ImageJ software and normalized with the levels of GAPDH. DMSO, Dimethyl sulfoxide; GAPDH, Glyceraldehyde 3-phosphate dehydrogenase; PARG, poly(ADP-ribose) glycohydrolase; PBMCs, peripheral blood mononuclear cells; PDO, patient-derived organoid; STAT3, signal transducer and activator of transcription 3.

with a significant decrease in IL-10, a pSTAT3-induced[35] cytokine known for its immunosuppressive properties[36] (figure 4C). These data, presented as mean-fold induction relative to control samples from three different HGSOC patients, confirm the role of PARG inhibition

in diminishing pSTAT3 and fostering an environment conducive to immune activation.

To further investigate the impact of PARG inhibition on T cell activation, we cocultured patient-derived tumor organoids or OVCAR8 spheroids with healthy donor

PBMCs. After 2 weeks, T-cell reactivity was analyzed by staining for the activation marker (granzyme B) and the degranulation marker (CD107a), both of which are indicators of cytotoxic T cell activity[30 37] (figure 4D). Flow cytometric analysis of the cocultures showed that 10 µM PARGi or 20 µg/mL PS-PARG antibody treatments for 72 hours, compared with their controls, significantly upregulated T cell activation markers in tumor organoid and OVCAR8 cocultures (figure 4E,F). These findings suggest that targeting PARG can boost T cell-mediated antitumor immunity.

PARG inhibition activates antitumor immune responses and CD8+ T cell-mediated antitumor effects in vivo

In our study, we explored the effects of PARG inhibition on antitumor immune responses in vivo. Female C57BL/6 mice were subcutaneously injected with Brca1-null ID8 mouse ovarian tumor cells, which mimic DDR-deficient human HGSOC.[24] The tumor-bearing mice were treated with either vehicle or COH34 (20 mg/kg) for 7 days.

Single-cell suspensions were prepared from mouse tumors and analyzed by immunoblotting and flow cytometry. The results showed that administration of COH34 led to a significant decrease in pSTAT3 in Brca1-null ID8 tumors and tumor-draining lymph nodes (online supplemental figure 4), as well as in CD45+ tumor-infiltrating immune cells (figure 5A, p<0.01). To gain further insight into the effect of PARG blockade on immune responses, regulatory T (Treg) and activated CD8+ T cells were assessed using flow cytometric analysis of tumor-derived single-cell suspensions. This analysis revealed a notable decrease in FoxP3+ Treg cells (figure 5B, p<0.05). Concurrently, there was a significant increase in CD8+ T cell activation markers, IFNγ, granzyme B, and CD69 (figure 5C–E), indicating a shift toward a more activated CD8+ T cell immune response following PARG blockade. To further test whether PARG inhibition-induced antitumor effect is contributed by CD8+ T cell activation, we depleted CD8+ T cells in C57BL/6 mice using neutralizing anti-CD8
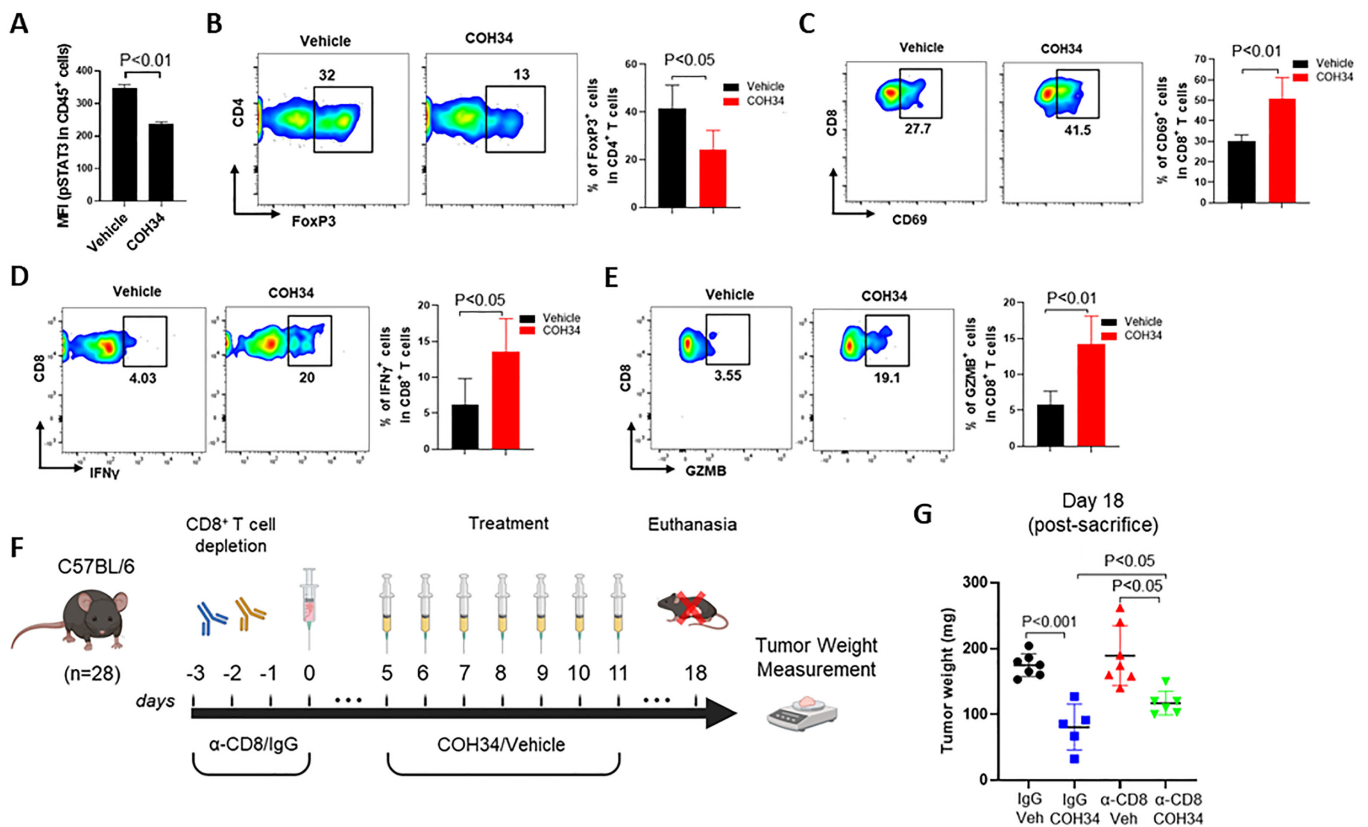
Figure 5 In vivo PARG inhibition induces antitumor immune responses, and the antitumor effects are partially mediated by CD8+ T cells. 5×10^6 Brca1-null ID8 tumor cells were injected subcutaneously into female C57BL/6 mice aged 7–10 weeks old. The tumor-bearing mice were treated with vehicle or COH34 (20 mg/kg) every day for 7 days. Single-cell suspensions prepared from the tumors were analyzed by flow cytometry to detect: (A) phosphorylated STAT3 (pSTAT3) in CD45+ immune cells. (B) FoxP3+ Tregs in CD4+ T cells and; (C, D, E) activated CD8+ T cells (CD69+ cells, IFN-γ+, and GZMB+). Data are shown as means±SD (n=4–5, each sample was pooled from 3 to 4 mice). (F) In vivo study design for (G). To deplete CD8+ T cells, C57BL/6 mice were injected intraperitoneally with rat anti-CD8 antibody or rat IgG2b (isotype control) on days −3 to −2, −1, and 0 relative to subcutaneous injection of Brca1-null ID8 tumor cells (day 0). When the tumors reached an average size of 100 mm³ on day 5, vehicle or COH34 (20 mg/kg) were administered by intraperitoneal injections every day for 7 days. (G) On day 18, mice were euthanized and tumor weight was measured. Data are shown as means±SD (n=5–7 mice per group). PARG, poly(ADP-ribose) glycohydrolase; STAT3, signal transducer and activator of transcription 3.

antibodies prior to tumor initiation (figure 5F). Consistent with a previous study,[20] COH34 treatment induced a significant inhibition of tumor growth after 1 week of intraperitoneal injections (20 mg/kg) compared with the control vehicle-treated group (figure 5G, p<0.001). Notably, depleting CD8^{+} T cells partially abrogated COH34-mediated tumor growth inhibition (p<0.05), suggesting that CD8^{+} T cells play a role in COH34-mediated tumor growth inhibition. Therefore, our findings collectively show that PARG inhibition in vivo can inhibit pSTAT3, activate antitumor immune responses and reduce tumor growth, which is partially dependent on CD8^{+} T cells.

DISCUSSION

Recurrent ovarian cancer remains a significant challenge due to its high mortality rate and limited treatment options after standard therapy. Although PARPis are highly promising in DDR-deficient ovarian cancer through synthetic lethality of tumor cells, resistance to PARPi eventually develops. It has been reported that inhibiting PARP can induce immunosuppression through increasing pSTAT3.[10 11] Like targeting PARP, PARG inhibition kills tumor cells through regulating DDR. However, unlike PARPi, this study shows that PARG inhibition effectively reduces pSTAT3 levels across various models, including ovarian tumor cell lines, patient tumor-derived organoids, and mouse ovarian tumors in vivo, as well as in immune cells, including patient ascites-derived T cells. By inhibiting pSTAT3, PARG targeting leads to additional antitumor effects through direct tumor cell killing and activating antitumor immune responses, highlighting the potential of PARG as an effective target for ovarian cancer treatment.

PARG targeting is shown to impair epithelial-to-mesenchymal transition (EMT) through vimentin and fibronectin 1 downregulation.[38] Another study revealed that PARG inhibition leads to tumor cell death by causing c-MYC destabilization through DDB1-dependent modulation.[39] STAT3 plays a critical role in promoting EMT and expression of vimentin and fibronectin 1, as well as c-MYC.[40–42] EMT and c-MYC are crucial players in cancer development, as EMT facilitates cancer cell invasion, metastasis, and resistance to therapies,[43] while c-MYC acts as a potent oncogene, regulating tumor cell proliferation, survival, and cancer metabolism, thereby driving tumor growth and progression.[44] A critical role of STAT3 in promoting tumor cell proliferation, survival and reprogramming cancer metabolism is known.[45] Therefore, some of the reported antitumor effects induced by PARG inhibition may be mediated partially by the blockade of pSTAT3.

We showed that tumor cell growth inhibition by PARGi is partially mediated by reduced STAT3 activity. Given that PARG inhibitors can downregulate pSTAT3 in both BRCA-deficient and proficient cells, our results suggest that the antitumor effects of PARG inhibitors might

extend beyond DDR-deficient tumors. Increased pSTAT3 could promote PARPi resistance in ovarian cancer cell lines and patient tumors.[10 11] Since PARG blockade suppressed pSTAT3 in cancer cells in vitro and in vivo, it is plausible that PARG targeting may mitigate PARPi resistance and potentially resensitize tumor cells to PARPi treatments. Further research is necessary to delineate the mechanisms and validate the therapeutic potential of PARGis in overcoming PARPi resistance. Accumulating evidence suggests that persistent STAT3 activation is a key contributor to the development of therapeutic resistance to various anticancer drugs,[46–48] including standard first-line chemotherapeutic agents in the clinical treatment of ovarian cancer, such as platinum-based chemotherapy and paclitaxel.[49 50] Considering its critical role in driving therapeutic resistance, targeting STAT3 signaling through PARG inhibition may be a promising strategy to overcome drug resistance and improve the clinical outcomes of patients with cancer.

Our study highlights the importance of PARG inhibition in modulating the tumor immunological microenvironment. STAT3 activity in immune cells has a critical role in compromising antitumor immune responses.[13–16] Here, we show that by decreasing pSTAT3 in immune cells, PARG inhibitors can activate antitumor immune responses in vitro and in vivo. This dual mechanism of inducing antitumor effects positions PARG as a promising therapeutic target for cancer treatment, including enhancing immunotherapy effectiveness. In line with our findings, previous research demonstrated that combining PARG inhibition with immune checkpoint blockade therapy significantly enhanced antitumor efficacy in a hepatocellular carcinoma model.[39] Although the mechanisms underlying the interplay between PARG inhibition and immune cell activation remain to be further investigated, our study supports the clinical development of PARG inhibitors for cancer treatments, including combination therapy with immunotherapy agents, in ovarian cancer and other malignancies.

Author affiliations
[1]Department of Immuno-Oncology, City of Hope Comprehensive Cancer Center, Duarte, California, USA
[2]Department of Surgery, City of Hope National Medical Center, Duarte, California, USA
[3]City of Hope Irell & Manella Graduate School of Biological Sciences, Duarte, California, USA
[4]Department of Cancer Genetics and Epigenetics, City of Hope Comprehensive Cancer Center, Duarte, California, USA
[5]Department of Medical Oncology and Therapeutics Research, City of Hope National Medical Center, Duarte, California, USA

Contributors These authors contributed equally: AM and CZ. AM and HY conceived the study. AM, CZ and HY designed experiments and interpreted data. AM and HY wrote the manuscript. AM, CZ, TA, Y-JL, RH, NLS, AK, QZ and RMB performed and analyzed experiments. NLS, MS and LR-R provided patient samples. LR-R also

ORCID iDs
Yi-Jia Li http://orcid.org/0000-0002-8791-8097
Hua Yu http://orcid.org/0000-0003-0931-1000

REFERENCES

1. Matulonis UA, Sood AK, Fallowfield L, *et al*. Ovarian cancer. *Nat Rev Dis Primers* 2016;2:16061.
2. Siegel RL, Miller KD, Wagle NS, *et al*. Cancer statistics, 2023. *CA Cancer J Clin* 2023;73:17–48.
3. Morand S, Devanaboyina M, Staats H, *et al*. Ovarian cancer Immunotherapy and personalized medicine. *Int J Mol Sci* 2021;22:6532.
4. Drakes ML, Stiff PJ. Ovarian cancer: therapeutic strategies to overcome immune suppression. *Adv Exp Med Biol* 2021;1330:33–54.
5. Fucikova J, Coosemans A, Orsulic S, *et al*. Immunological configuration of ovarian carcinoma: features and impact on disease outcome. *J Immunother Cancer* 2021;9:e002873.
6. Bryant HE, Schultz N, Thomas HD, *et al*. Specific killing of Brca2-deficient tumours with inhibitors of Poly(ADP-ribose) polymerase. *Nature* 2005;434:913–7.
7. Farmer H, McCabe N, Lord CJ, *et al*. Targeting the DNA repair defect in BRCA mutant cells as a therapeutic strategy. *Nature* 2005;434:917–21.
8. Lee CK, Friedlander ML, Tjokrowidjaja A, *et al*. Molecular and clinical predictors of improvement in progression-free survival with maintenance PARP inhibitor therapy in women with platinum-sensitive, recurrent ovarian cancer: A meta-analysis. *Cancer* 2021;127:2432–41.
9. Dias MP, Moser SC, Ganesan S, *et al*. Understanding and overcoming resistance to PARP inhibitors in cancer therapy. *Nat Rev Clin Oncol* 2021;18:773–91.
10. Ding L, Wang Q, Martincuks A, *et al*. STING Agonism overcomes Stat3-mediated immunosuppression and adaptive resistance to PARP inhibition in ovarian cancer. *J Immunother Cancer* 2023;11:e005627.
11. Martincuks A, Song J, Kohut A, *et al*. PARP inhibition activates Stat3 in both tumor and immune cells underlying therapy resistance and immunosuppression in ovarian cancer. *Front Oncol* 2021;11:724104.
12. Ding L, Chen X, Xu X, *et al*. Parp1 suppresses the transcription of PD-L1 by Poly(ADP-Ribosyl)Ating Stat3. *Cancer Immunol Res* 2019;7:136–49.
13. Wang T, Niu G, Kortylewski M, *et al*. Regulation of the innate and adaptive immune responses by Stat-3 signaling in tumor cells. *Nat Med* 2004;10:48–54.
14. Kortylewski M, Kujawski M, Wang T, *et al*. Inhibiting Stat3 signaling in the hematopoietic system elicits Multicomponent antitumor immunity. *Nat Med* 2005;11:1314–21.
15. Yu H, Kortylewski M, Pardoll D. Crosstalk between cancer and immune cells: role of Stat3 in the tumour Microenvironment. *Nat Rev Immunol* 2007;7:41–51.
16. Zou S, Tong Q, Liu B, *et al*. Targeting Stat3 in cancer Immunotherapy. *Mol Cancer* 2020;19:145.
17. Pascal JM, Ellenberger T. The rise and fall of Poly(ADP-ribose): an enzymatic perspective. *DNA Repair (Amst)* 2015;32:10–6.
18. Kassab MA, Yu LL, Yu X. Targeting dePARylation for cancer therapy. *Cell Biosci* 2020;10:7.
19. Houl JH, Ye Z, Brosey CA, *et al*. Selective small molecule PARG inhibitor causes replication fork stalling and cancer cell death. *Nat Commun* 2019;10:5654.
20. Chen SH, Yu X. Targeting dePARylation selectively suppresses DNA repair-defective and PARP inhibitor-resistant malignancies. *Sci Adv* 2019;5:eaav4340.
21. Zhang W, Zhang C, Li W, *et al*. Cd8+ T-cell Immunosurveillance constrains Lymphoid Premetastatic myeloid cell accumulation. *Eur J Immunol* 2015;45:71–81.
22. Kopper O, de Witte CJ, Lõhmussaar K, *et al*. An Organoid platform for ovarian cancer captures Intra- and Interpatient heterogeneity. *Nat Med* 2019;25:838–49.
23. Neal JT, Li X, Zhu J, *et al*. Organoid modeling of the tumor immune Microenvironment. *Cell* 2018;175:1972–88.
24. Ding L, Kim H-J, Wang Q, *et al*. PARP inhibition elicits STING-dependent antitumor immunity in Brca1-deficient ovarian cancer. *Cell Rep* 2018;25:2972–80.
25. Stordal B, Timms K, Farrelly A, *et al*. Brca1/2 Mutation analysis in 41 ovarian cell lines reveals only one functionally deleterious Brca1 Mutation. *Mol Oncol* 2013;7:567–79.
26. Kondrashova O, Topp M, Nesic K, *et al*. Methylation of all Brca1 copies predicts response to the PARP inhibitor Rucaparib in ovarian carcinoma. *Nat Commun* 2018;9:3970.
27. Herrmann A, Nagao T, Zhang C, *et al*. An effective cell-penetrating antibody delivery platform. *JCI Insight* 2019;4:e127474.
28. Bromberg JF, Wrzeszczynska MH, Devgan G, *et al*. Stat3 as an Oncogene. *Cell* 1999;98:295–303.
29. Burke JD, Young HA. IFN-Γ: A cytokine at the right time, is in the right place. *Semin Immunol* 2019;43:101280.
30. Tibbs E, Cao X. Emerging Canonical and non-Canonical roles of Granzyme B in health and disease. *Cancers (Basel)* 2022;14:1436.
31. Zhang C, Yue C, Herrmann A, *et al*. Stat3 activation-induced fatty acid oxidation in Cd8(+) T Effector cells is critical for obesity-promoted breast tumor growth. *Cell Metab* 2020;31:148–61.
32. Kujawski M, Zhang C, Herrmann A, *et al*. Targeting Stat3 in Adoptively transferred T cells promotes their in vivo expansion and antitumor effects. *Cancer Res* 2010;70:9599–610.
33. Ichiba M, Nakajima K, Yamanaka Y, *et al*. Autoregulation of the Stat3 gene through cooperation with a cAMP-responsive element-binding protein. *J Biol Chem* 1998;273:6132–8.
34. Narimatsu M, Maeda H, Itoh S, *et al*. Tissue-specific Autoregulation of the Stat3 gene and its role in Interleukin-6-induced survival signals in T cells. *Mol Cell Biol* 2001;21:6615–25.
35. Kinjyo I, Inoue H, Hamano S, *et al*. Loss of Socs3 in T helper cells resulted in reduced immune responses and Hyperproduction of interleukin 10 and transforming growth factor-beta 1. *J Exp Med* 2006;203:1021–31.
36. Dennis KL, Blatner NR, Gounari F, *et al*. Current status of Interleukin-10 and regulatory T-cells in cancer. *Curr Opin Oncol* 2013;25:637–45.
37. Betts MR, Brenchley JM, Price DA, *et al*. Sensitive and viable identification of antigen-specific Cd8+ T cells by a flow Cytometric assay for Degranulation. *J Immunol Methods* 2003;281:65–78.
38. Marques M, Jangal M, Wang L-C, *et al*. Oncogenic activity of poly (ADP-ribose) Glycohydrolase. *Oncogene* 2019;38:2177–91.
39. Yu M, Chen Z, Zhou Q, *et al*. PARG inhibition limits HCC progression and potentiates the efficacy of immune Checkpoint therapy. *J Hepatol* 2022;77:140–51.
40. Carpenter RL, Lo HW. Stat3 target genes relevant to human cancers. *Cancers (Basel)* 2014;6:897–925.
41. Deng J, Liu Y, Lee H, *et al*. S1Pr1-Stat3 signaling is crucial for myeloid cell Colonization at future metastatic sites. *Cancer Cell* 2012;21:642–54.
42. Jin W. Role of JAK/Stat3 signaling in the regulation of metastasis, the transition of cancer stem cells, and Chemoresistance of cancer by epithelial-Mesenchymal transition. *Cells* 2020;9:217.

43 Nieto MA, Huang RY-J, Jackson RA, *et al*. Emt: 2016. *Cell* 2016;166:21–45.

44 Dang CV. MYC on the path to cancer. *Cell* 2012;149:22–35.

45 Li YJ, Zhang C, Martincuks A, *et al*. STAT proteins in cancer: orchestration of metabolism. *Nat Rev Cancer* 2023;23:115–34.

46 Lee H-J, Zhuang G, Cao Y, *et al*. Drug resistance via feedback activation of Stat3 in Oncogene-addicted cancer cells. *Cancer Cell* 2014;26:207–21.

47 Martincuks A, Li P-C, Zhao Q, *et al*. Cd44 in ovarian cancer progression and therapy resistance-A critical role for Stat3. *Front Oncol* 2020;10:589601.

48 Zhao C, Li H, Lin H-J, *et al*. Feedback activation of Stat3 as a cancer drug-resistance mechanism. *Trends Pharmacol Sci* 2016;37:47–61.

49 Yue P, Zhang X, Paladino D, *et al*. Hyperactive EGF receptor, Jaks and Stat3 signaling promote enhanced colony-forming ability, motility and migration of cisplatin-resistant ovarian cancer cells. *Oncogene* 2012;31:2309–22.

50 Sheng H, Feng Q, Quan Q, *et al*. Inhibition of Stat3 reverses Taxol-resistance in ovarian cancer by down-regulating G6Pd expression in vitro. *Biochem Biophys Res Commun* 2022;617(Pt 2):62–8.